Measurement of Antenna System Noise Temperature Using Planar Near-Field Data

A.C. Newell[#1], P. Pelland[#2], S.F. Gregson[#3], D. Janse Van Rensburg[#4]
1125 Satellite Blvd., Suite 100
Suwanee, GA 30024-4629 USA
[1]anewell@nsi-mi.com
[2]ppelland@nsi-mi.com
[3]sgregson@nsi-mi.com
[4]drensburg@nsi-mi.com

***Abstract*—This paper presents the results of a new measurement technique to determine antenna system noise temperature using data acquired from a planar near-field measurement. The ratio of antenna gain to system noise temperature (G/T) is usually determined in a single measurement when the antenna is alternately pointed towards the "cold sky" and a hot radio source such as the sun or a star with a known flux density. The antenna gain is routinely determined from near-field measurements and with the development of this new technique, the system noise temperature can also be determined using the same measurements. The ratio of G/T can therefore be determined from planar near-field data without moving the antenna to an outdoor range. The noise temperature is obtained by using the plane-wave spectrum of the planar near-field data and focusing on the portion of the spectrum in the evanescent or "imaginary space" portion of the spectrum. Near-field data is obtained using a data point spacing of λ/4 or smaller and the plane-wave spectrum is calculated without applying any probe correction or Cos(θ) factor. The spectrum is calculated over real space corresponding to propagating modes of the far-field pattern and also the evanescent or imaginary space region where $k_x^2 + k_y^2 \geq k^2$. Actual evanescent modes are highly attenuated in the latter region and therefore the spectrum in this region must be produced by "errors" in the measured data. Some error sources such as multiple reflections will produce distinct localized lobes in the evanescent region and these are recognized and correctly identified by using a data point spacing of less than λ/2 to avoid aliasing errors in the far-field pattern. It has been observed that the plane wave spectrum beyond these localized lobes becomes random with a uniform average power. This region of the spectrum must be produced by random noise in the near-field data that is produced by all sources of thermal noise in the electronics and radiated noise sources received by the antenna. By analysing and calibrating this portion of the spectrum in the evanescent region the near-field noise power can be deduced and the corresponding noise temperature determined. Simulated and measured data will be presented to illustrate and validate the measurement and analysis techniques.**

Keywords—Planar Near-Field, Noise Temperature, G/T Figure-of-Merit Measurements, Simulation, Plane Wave Spectrum.

I. INTRODUCTION

A receiving antenna system can be modeled as shown in Figure 1 by the antenna with a gain of G, an ohmic loss of α, an amplifier with a gain denoted by A and the noise figure of the amplifier denoted as F.

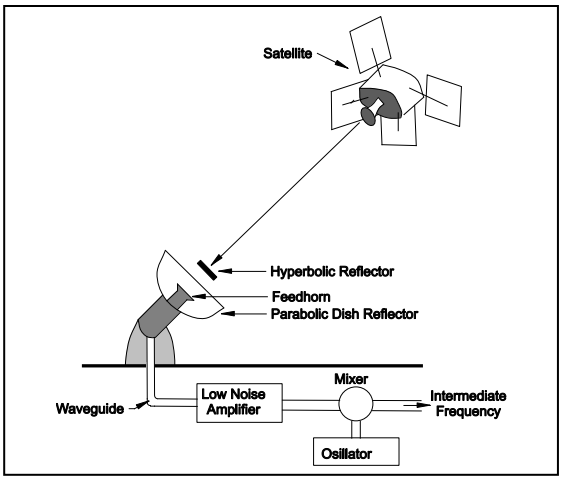

Figure 1 Antenna Receiving system schematic.

A frequently used figure of merit for the receiving system is the ratio of the antenna gain, G to the effective noise temperature of the antenna and amplifier T_e. The effective noise temperature of the system is due to the noise produced by the antennas ohmic loss that is directly related to the radiation efficiency η and the amplifier noise. This figure of merit is usually measured by alternately directing the antenna towards a hot noise source such as the sun, moon or radio star and then towards a "cold" region of space that is free of noise sources other than the cosmic background radiation. From the measured change in the received noise of the antenna system and knowledge of the noise temperature of the hot and cold noise sources, the ratio of G/T_e can be determined. A large disadvantage of this technique for a satellite antenna system is the need to transport and place the satellite in an outdoor environment where it can be directed towards the hot and cold radiation sources. Since the satellite with all of its antennas and electronic systems has been assembled and tested in a controlled clean environment, exposure to an outdoor range could cause damage or contamination of sensitive components.

Near-Field measurement techniques have been developed, proven and are routinely used for the accurate measurement of antenna pattern, gain, directivity, polarization, EIRP and Saturating Flux Density [1, 2]. Work is currently underway to develop and implement near-field measurements to determine system group delay and End-to-End testing of satellite communication systems. With these developments and the successful implementation of the measurement of satellite system noise that will be described in the following paper, all of the communication satellite testing could be performed on a near-field range without the need to move to any other far-field or compact range. This would greatly reduce the time, cost and complexity of the testing process and avoid potential problems associated with the transportation and hazards of other measurement environments.

II. Proposed Measurement and Analysis

The measurement and analysis technique for determining antenna noise and the ratio of gain to noise temperature that will be described in the following sections is very different than traditional approaches. The first difference is that the antenna gain and noise temperature are determined separately rather than as a ratio. Both of these parameters are derived from the analysis of planar near-field measurements but the details are different for the two parameters. The second difference is that neither hot nor cold noise standards are required and the measurement system and processing are based on a total power radiometer concept where the noise power is measured relative to an absolute scale in milliwatts.

The determination of gain from planar near-field measurements is a standard process that is well established and will not be reviewed in this paper. The uncertainty in antenna gain will depend on the gain standard and the measurement process, and is typically on the order of ±0.1 to ±0.5 dB. Directivity is also routinely available from the near-field measurements and processing. The radiation efficiency η and therefore ohmic loss of the antenna are easily obtained from the difference between gain and directivity. The other part of thermal noise in the antenna system is due to the electronic components used to amplify and detect the RF signal. These can be measured before the electronics are installed in the antenna system using standard noise figure measurements, but it is usually desirable to also perform a measurement on the assembled system, and that is the goal of the following proposed technique.

In a planar near-field measurement where the AUT is receiving, the amplitude and phase of the AUT output signal is measured at equally spaced points in x and y as the probe moves over a planar surface where the z-distance is constant. In an ideal measurement, the AUT output is produced by the radiating field of the probe coupling with the receiving properties of the AUT and the transmission equation describing this interaction is shown in (1).

$$b_{Ap}(x,y,d) = F' a_0' \iint \vec{t}_{01}(\vec{K}) \bullet \vec{s}_{20}'(\vec{K}) e^{i\gamma d} e^{i(k_x x + k_y y)} dk_x dk_y$$

where

$b_{Ap}(x,y,d)$ = **the ideal output signal of the AUT due to Probe/AUT coupling with no measurement errors**

$\vec{t}_{01}(\vec{K})$ = **the receiving spectrum of the AUT**

$\vec{s}_{20}'(\vec{K})$ = **the transmitting spectrum of the probe**

F' = **a mismatch factor due to the impedance of the AUT and the receiver connected to the AUT**

(k_x, k_y, γ) = **the components of the plane wave propagating vector $\vec{k}$**

a_0' = **input signal to the probe** (1)

In an actual measurement, the total signal detected and recorded by the near-field measurement system is the sum of the ideal probe/AUT coupling component and a number of terms due to errors in the measurement system.

$$b_T(x,y,d) = b_{Ap}(x,y,d) + \sum_i \varepsilon_i(x,y,d)$$

where

$\varepsilon_i(x,y,d)$ = **error terms due to imperfections in the measurement system** (2)

The sources of the individual error terms have been identified [3] through a study referred to as the NIST 18 Term Error Analysis. The sources that produce errors in the measured data are AUT alignment, data point spacing, x, y and z position errors, mutual coupling, receiver amplitude and phase non-linearity, receiver dynamic range, room scattering, cable and rotary joint errors, leakage and random errors. With the exception of the last term, all of the others are systematic and their plane wave spectrum is band limited. Due to the attenuation of the evanescent plane waves transmitted by the probe and received by the AUT, the plane wave spectrum of the probe/AUT term is also band limited. If planar measurements are performed at increments in x and y less than λ/8 and the plane-wave spectrum of the measured data computed as shown in (3)

$$D_T(k_x, k_y) = \frac{e^{-i\gamma d}}{4\pi^2} \int b_T(x,y,d) e^{-i(k_x x + k_y y)} dx dy, \quad (3)$$

the spectrum for propagating modes in real space and the modes in the evanescent region or imaginary space can be represented as shown in Figure 2. The spectrum within the unit circle where

$$\frac{k_x^2 + k_y^2}{k^2} \le 1.0 \quad (4)$$

is primarily due to the ideal probe/AUT coupling term and if there were no measurement errors, the spectrum should decay exponentially beyond the unit circle. The distinct localized lobes along the lines

$$\frac{k_x}{k} = \pm 1.2 \text{ and at } \frac{k_x}{k} = 0, \ \frac{k_y}{k} = \pm 1.2 \quad (5)$$

for the measurement shown in Figure 2 are known to be due to the modulation of the multiple reflection signals with a period associated with the spacing of the elements in a slotted array AUT. Similar localized lobes are observed for other antennas but may be at other locations in k-space. The origin of the "shadow" spectrum close to the principal planes has not been identified, but could be due to truncation, multiple reflections or room scattering. It is not necessary for the present purposes to identify the source of this part of the spectrum but it is apparent in some form in all measurements. This shadow characteristic is band limited and does not contribute to the spectrum beyond limits that can be determined from observation of graphic representation like Figure 2.

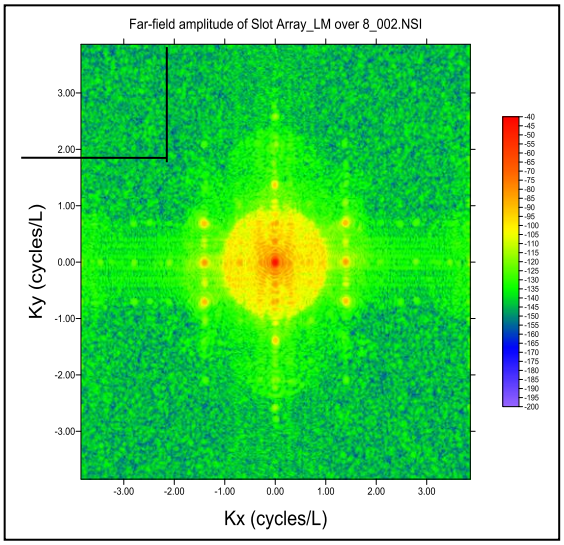

Figure 2 Plane-wave spectrum of data measured with a data point spacing of λ/8.

Beyond the limits of the distinct lobes and the shadow region, the plane wave spectrum becomes relatively uniform and if measurements are performed using even smaller increments; the level of the spectrum does not decrease. The source of this part of the spectrum must be a random error signal cause by thermal noise in the measured data because only thermal noise can produce a uniform spectrum without a band limit. If this portion of the spectrum can be used to determine the near-field signal on an absolute level that would produce the observed spectrum, the thermal noise in the measurement system can be determined. The following sections will discuss the steps in the process to determine the thermal noise level.

III. Steps in the Analsis

The first step in the analysis is to calculate and display the plane-wave spectrum of the data measured with a spacing of λ/8 as shown in Figure 2. A custom software script is used in each of the processing steps and the user first selects a uniform region of k-space by specifying the minimum and maximum values of k_x and k_y for a rectangular area where the amplitude is uniform and free of any localized lobes or "shadow" features such as the upper left corner of Figure 2 and shown expanded in Figure 3.

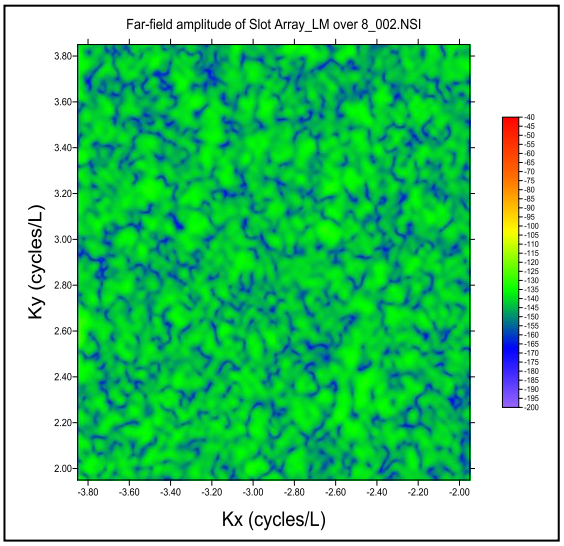

Figure 3 Selected region of the plane wave spectrum with uniform amplitude.

The power of the spectrum within this partial region of k-space is then calculated

$$PS_P = \frac{\Delta k_x \Delta k_y}{4\pi^2} \sum_{k_x\,\min}^{k_x\,\max} \sum_{k_y\,\min}^{k_y\,\max} \left| D_T(k_x, k_y) \right|^2 \qquad (6)$$

The thermal noise spectrum extends uniformly over all k-space but is obscured by the spectrum of the AUT and other errors, but since it is uniform, its total power over all calculated k-space can be determined from the total power over the selected region and a span correction. The span correction is the ratio of the total number of data points over all calculated k-space to the number of points within the selected region.

$$Span\,Correction = \frac{NT_x NT_y}{NS_x NS_y} \qquad (7)$$

In (7), NT_x and NT_y are respectively the total number of spectral points in calculated k-space; NS_x and NS_y are respectively the number of spectral points in the selected region of k-space. The total power over all calculated k-space is then

$$PS_T = PS_P(Span\ Correction). \qquad (8)$$

Using Parseval's theorem [4], the total power in the spectral domain is equal to the total power in the near-field measured data and therefore, the total and average power of the thermal noise in the measured data are respectively

$$PNF_T = PS_T \qquad PNF_A = \frac{PNF_T}{N_x N_y}. \qquad (9)$$

N_x and N_y are respectively the number of x and y data points in the near-field data array. The measured near-field

data is recorded as the ratio between the reference channel and the measurement channel of the receiver. The amplitude scales in Figures 2 and 3 have used near-field data as measured relative to the reference channel. The measurement menu in the software also records the absolute power level of the reference channel in dBm. When this reference power level is applied as a correction to the power quantities in (9) they become absolute power levels calibrated in dBm. The thermal noise temperature of the antenna and measurement system can then be calculated using the relationship

$$PNF_A = KTB \tag{10}$$

In (10), K is Boltzmann's constant; T is the system noise temperature in Kelvin; B is the receiver bandwidth in reciprocal seconds.

IV. Simulation to Test Analysis

The proposed measurement and analysis for determining system noise temperature were tested using two kinds of simulated near-field data where a known system noise temperature or noise power could be imposed on ideal near-field data. The simulated data was then processed using the script described in the previous section and the calculated noise power or temperature compared with the input values. Using this process, the script, analysis and software used in the measurement and data processing could be checked.

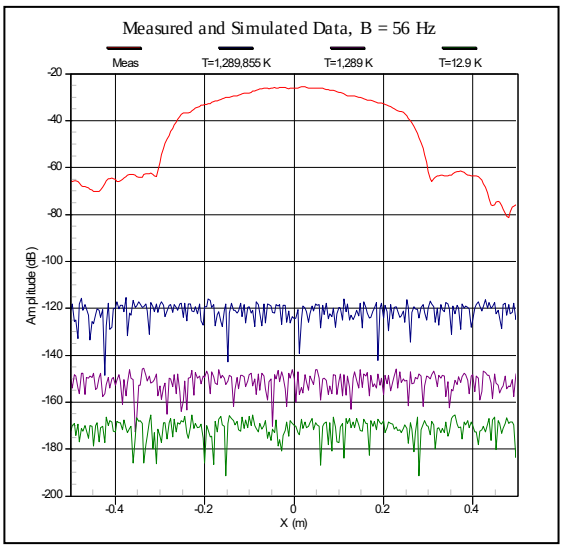

Figure 4 Measured and simulated near-field data.

In Figures 4 and 5, the amplitude scale is referenced to one milliwatt.

The first simulation replaced all the measured data with random amplitude and phase with a specified average power. Figure 4 shows X-cuts of the measured and simulated noise data with noise power levels of -120, -150 and -170 dBm. For a receiver bandwidth of 56 Hz, these noise powers correspond respectively to noise temperatures of 1289855, 1289 and 12.9 K. The plane wave spectrum of the simulated data had uniform amplitude as expected and the processing could use either the full computed k-space or different partial regions to calculate near-field noise power. Table 1 shows the results for the three power levels computed using different partial regions.

Table 1 Results of simulation using uniform noise for near-field data.

INPUT NOISE (dBm)	K_x MIN	K_x MAX	K_y MIN	K_y MAX	CALCULATED OUTPUT NOISE (dBm)
-120	-4	4	-4	4	-120.02
-120	-4	-1	1	4	-120.07
-150	-4	4	-4	4	-150.01
-150	1	4	-4	1	-149.97
-170	-4	4	-4	4	-170.01
-170	-4	-1	-4	-1	-170.01

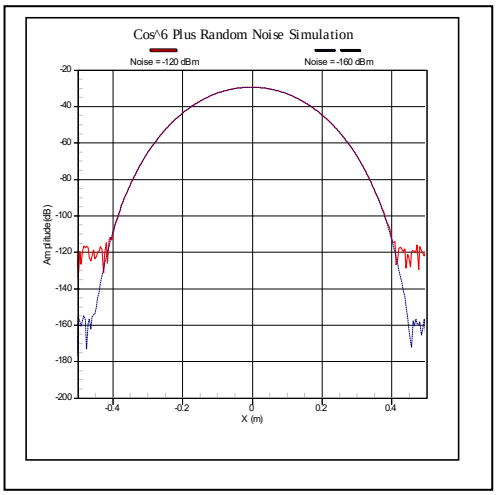

Figure 5 Simulated near-field data plus random noise.

For the second simulation, the measured data is replaced by a near-field amplitude distribution with a smooth variation in x and y and very low truncation. A prescribed noise level is then added to the amplitude data as shown in (11) and illustrated in Figure 5 when n = 6 and two noise levels are shown.

$$b_T(x,y) = \cos^n\left(\frac{2\pi x}{L_x}\right)\cos^n\left(\frac{2\pi y}{L_y}\right) + Noise \tag{11}$$

Table 2 Results of simulation with simulated antenna data plus random noise.

INPUT NOISE (dBm)	K_x MIN	K_x MAX	K_y MIN	K_y MAX	CALCULATED OUTPUT NOISE (dBm)
-120	-4	4	1	4	-119.99
-160	-4	4	1	4	-159.96

The results of both types of simulation verify that the process is sound, the dynamic range and resolution of the processing software is sufficient to analyze the low noise levels and the processing script can determine absolute system noise power accurately over a very large dynamic range that is larger than expected in an actual measurement.

V. Measurements and Analysis of System with Known Noise Properties

The next step in the demonstration and verification of this purposed technique is to perform actual planar near-field measurements on an antenna and receiving system with known noise parameters. This requires measurement of the noise figure for the amplifiers and receivers in the system and knowledge of the noise temperature of the antenna field of view during the measurement. These measurements are being performed and the results will be reported in the presentation at the conference.

VI. Conclusions

A new technique for measuring antenna noise and G/T has been described, illustrated and verified with simulations. The technique uses planar near-field measurements performed to measure other antenna parameters and greatly reduces the time and complexity of these measurements. Further tests will be done to develop and refine this technique so it can be implemented for complete system testing.

References

[1] Newell, A.C.; Ward, R.D.; McFarlane, E.J., "Gain and Power Parameter Measurements Using Planar Near-Field Techniques," *IEEE Transactions on Antennas and Propagation, Vol.* AP-36, No. 6, pp. 792-803, June 1988.

[2] D.J. Janse van Rensburg & K. Haner, "EIRP & SFD measurement methodology for planar near-field antenna ranges", AMTA 36th Annual Meeting & Symposium, Tucson, AZ, USA, Oct. 2014.

[3] Newell, A.C., "Error analysis techniques for planar near-field measurements," *IEEE Transactions on* Antennas and *Propagation, Vol.* AP-36, pp. 755-768, June 1988.

[4] Parseval des Chênes, Marc-Antoine Mémoire sur les séries et sur l'intégration complète d'une équation aux différences partielles linéaire du second ordre, à coefficients constants" presented before the Académie des Sciences (Paris) on 5 April 1799. This article was published in *Mémoires présentés à l'Institut des Sciences, Lettres et Arts, par divers savants, et lus dans ses assemblées. Sciences, mathématiques et physiques. (Savants étrangers.)*, vol. 1, pages 638–648 (1806).